Layered Double Hydroxide (LDH)-Derived Mixed Metal Oxides (MMOs)

Materials Science inc. Nanomaterials & Polymers

Layered Double Hydroxide (LDH)-Derived Mixed Metal Oxides (MMOs): A Systematic Crystal-Chemical Approach to Investigating the Chemical Composition and its Effect on High Temperature CO_2 capture.

Li Anne Cheah, G. V. Manohara, M. Mercedes Maroto-Valer, and Susana Garcia*[a]

A systematic study was conducted to establish a chemically meaningful relationship between the chemical composition of precursor, layered double hydroxide (LDH) and the CO_2 uptake capacities of the derived mixed-metal oxides (MMOs) sorbent. A simple crystal-chemical approach based on Vegard's law is proposed as a better characterization technique for LDHs, using lattice parameter *a* to find the true composition, *x*. Close values of *a* for all the resultant LDHs (3.051 - 3.056 Å) suggests a thermodynamic preference to produce LDHs having a composition that is close to that of mineral Hydrotalcite (3.054 Å). Solid state ^{27}Al spectra reveal the presence of aluminium based amorphous impurity phases in bulk LDHs. Due to the employed synthesis method and complex solution chemistry of the unitary hydroxides involved, it proved difficult to get the desired composition and to control the presence of impurities. The presence of remnant sodium has a significant effect on the CO_2 uptake capacities of the resultant MMOs. Overall, the choice of synthesis method, purity of the samples, presence of impurities and chemical efficiency of the whole synthesis process plays a major role on developing LDH based MMOs sorbents for CO_2 capture.

1. Introduction

Global warming is now recognized as the biggest global issue facing mankind and the cause is often related to the rising carbon dioxide (CO_2) concentration in the earth's atmosphere.[1] Carbon Capture and Storage (CCS) appears to be the current most viable technique to prevent large amount of anthropogenic CO_2 from being released into the atmosphere.[2] At present, absorption technology using liquid amine-based solvents is employed for capturing CO_2 at commercial scale. However, this technology still suffers from issues such as high energy cost, long regeneration time, materials degradation and release of toxic substances.[3] A potential better alternative is adsorption using solid sorbents which has the benefits of lower heat capacities, better capture capacity, cyclic stability, lesser waste generation and environmentally friendly. In addition, some solid sorbents, such as alkali and alkaline earth metal oxides (i.e. magnesium-based, lithium-based and calcium-based oxides) can be used at high capture temperatures (> 100 °C) eliminating the need to cool down the hot flue gases and further reducing the energy penalty.[4] Among the solid sorbents, layered double hydroxides (LDHs) show promising high-temperature CO_2 capture properties such as 1) relatively fast adsorption/desorption kinetics,[5] 2) lower regeneration energy, 3) ease of synthesis,[6] 4) environmentally benign, 5) good cyclic stability and 6) work well under moisture condition.[7]

LDHs, commonly known as hydrotalcite-like compounds, are a class of layered anionic clays with general formula $\left[M^{2+}_{1-x}M^{3+}_{x}(OH)_2\right]^{x+}[A^{m-}_{x/m}]^{x-}\cdot nH_2O$, where M^{2+} and M^{3+} are di- and trivalent cations and A^{m-} is the balancing anion at the interlayer. The *x* is the mole fraction of the trivalent cation and is often used to represent the chemical composition of LDHs. According to the Pauling's cation avoidance rule, this *x* should only be valid between 0.2 - 0.33 for pure LDH phase.[8] Generally, LDHs are synthesized by Miyata's co-precipitation method[9] but other methods such as urea hydrolysis,[10] hydrothermal,[11] memory effect[12] and anion exchange[13] are also adopted. Calcination of LDHs under inert/oxidizing environment leads to the formation of mixed metal oxides (MMOs) through the dehydration, dehydroxylation and deanation steps.[14] Due to the basic nature of the MMOs, they have been employed for high temperature CO_2 capture. Much attention has been given to Mg-based LDHs because of their unique adsorption-desorption temperature window (200 – 400 °C) which makes them suitable for specific flue gas conditions, i.e. pre-combustion and industrial processes.[15]

Like many other solid sorbents, the chemical composition of the precursor LDHs plays a vital role on the CO_2 capture performance of the derived MMOs. Mechanistic studies have

[a] L. A. Cheah, G. V. Manohara, M. M. Maroto-Valer, S. Garcia
Research Centre for Carbon Solutions (RCCS), School of Engineering and Physical Sciences
Heriot-Watt University
Edinburgh EH14 4AS (United Kingdom)
E-mail: s.garcia@hw.ac.uk

Supporting information for this article is available on the WWW under https://doi.org/10.1002/slct.201904447

confirmed that MgO is the active adsorbent species in the MMOs for CO_2 capture.[16] Hence, there should be a direct relationship between the composition of the LDHs and the CO_2 capture capacity of the resultant MMOs. However, such relationship is not observed so far in the literature and different studies have reported a different optimum LDHs composition. For instance, Yong *et al.* observed an optimal Al content of 50% for CO_2 capture which contradicts the 37% observed by Sharma *et al.* and is higher than the 22% reported by Gao *et al.*[16–17] In addition to this ambiguity, MMOs obtained from LDHs with the same composition and synthesized by the same method show huge differences in CO_2 capture capacities. For instance, for MMOs with an *x* value of 0.25 and synthesized by the co-precipitation method, CO_2 capture capacities at 200 °C as different as 0.30, 0.49 and 0.71 mmol/g were reported in literature.[14,17a, 18] Clearly, there is a disputable relationship between the reported chemical composition of the precursor LDHs and the CO_2 capture capacities of the resultant MMOs. Because of these discrepancies, it is important to establish a chemically meaningful relationship between precursor LDHs and derived MMOs to optimally develop high-temperature CO_2 capture sorbents based on LDHs.

Most of the studies in the literature derived their measured chemical compositions from the chemical/elemental analysis of the precursor LDHs. Establishing the composition using chemical analysis is straight forward for most of the solid sorbents but not for LDHs. LDHs show complex solution chemistry starting from their synthesis to applications (e.g. anion exchange reaction). The unitary hydroxides involved in the formation of the LDHs show wide differences among their physical properties such as pH of formation, solubility product, thermodynamic stabilities and amphoteric nature of the metal cation.[19] These differences in physical constants of constituent unitary hydroxides have a large say in the final composition of the LDHs. Also, the formation mechanism of LDHs is not clearly understood to date. Some reports suggest dissolution-reprecipitation (D–R) and others suggest topotactic as the mechanism involved during LDHs formation.[19c,20] The reaction mechanism involved could influence the composition of the resultant LDHs. In addition to this, the evidence of competing and parallel reactions such as formation of amorphous hydroxides/oxy-hydroxides[21] and leaching out of metal cations from the hydroxide lattice[22] taking place under the conditions employed for the LDH synthesis has been previously reported. Due to all those complex factors, it is difficult to establish a meaningful LDH composition by chemical analysis alone. For instance, elemental analysis of LDHs shows the amount of M^{2+} and M^{3+} ions present in a given sample but it doesn't distinguish between amorphous (as impurity) and crystalline phase. This will tend to give misleading compositions of the resultant LDHs.

Given the significance that LDHs and related materials gained in recent years within the fields of catalysis in general and high temperature CO_2 capture in particular, establishing the precise chemical composition is vital.[23] A chemically meaningful composition for LDHs could be established by using a combination of crystal-chemical approach and analytical techniques. The lattice parameter *a* is directly proportional to the isomorphous substitution of M^{2+} ion in the hydroxide lattice with the M^{3+} ion in the solution. In this work, we report the use of crystal-chemistry model to determine the true chemical composition of precursor LDHs, coupled with various other techniques such as Elemental Analysis and solid-state ^{27}Al NMR and correlate it with the CO_2 adsorption performance of resultant MMOs.

2. Results and Discussion

2.1. Characterization of LDHs and MMOs

The successful synthesis of Mg–Al-CO_3 LDHs using different nominal compositions are evidenced in the PXRD patterns (See Supporting Information Figure S1a) and the samples are labelled with the molar Mg: Al ratios used at synthesis. The sharp and intense diffraction peak at low angle yielding a *d*-spacing value of 7.6 Å ($2\theta = 11.5$ °) represents the average distance between hydroxide layers in the (*003*) plane of the LDH crystal system and is the characteristic value of carbonate anion intercalated LDHs.[23] The submultiple peak is seen at 3.8 Å ($2\theta = 23.5$ °). The 'saw-tooth' shaped reflections at higher angles ($2\theta = 60$ - 62 °) are assigned to (*110*) and (*113*) planes.[23] Among them, the peak with a *d*-spacing value of 1.5 Å ($2\theta = 60.5$ °) represents the average metal-oxygen (M–O) distance at the crystal lattice and two times this value gives the unit cell parameter *"a"* of LDHs ($a = 2 \times d_{110}$). This is similar to the unit cell parameter *a* of Brucite, $Mg(OH)_2$ as LDH is essentially Brucite having some of the Mg^{2+} ions replaced by Al^{3+} ions at the octahedral sites in the hydroxide layers. Besides LDHs, no other obvious crystallized phase is seen from the diffractograms.

Table 1 lists the *a*-parameter of all LDHs synthesized with different nominal compositions. All *a* values for LDHs synthesized is lower than the *a* value of Brucite (3.142 Å),[24] which shows the successful replacement of Mg^{2+} ions (0.72 Å) by smaller Al^{3+} ions (0.53 Å).[25] The fact that the values of *a* are decreasing with decreasing Mg: Al ratios suggests a progressive incorporation of Al^{3+} and is consistent with the Vegard's law.[26] This is supported by the decreasing d_{003} values, which suggests increased interactions between hydroxide layers and anion interlayers due to higher Al content.[23] Interestingly, the two samples synthesized with nominal Mg: Al ratios of 3 and 4, are shown to have almost identical *a* and d_{003} values, suggesting a similar chemical composition, *x*.

Further successful synthesis of carbonate-LDHs is confirmed by the FTIR spectra, as shown in Figure S1b. The characteristic

Table 1. Nominal composition and lattice parameters of LDHs with different Mg: Al ratios.

Nominal Mg: Al Ratios	$X_{nominal}$	*a* (Å)	d_{003} (Å)	$X_{crystal}$
2	0.33	3.051	7.647	0.28
3	0.25	3.055	7.673	0.27
4	0.20	3.056	7.674	0.27
5	0.17	3.070	7.812	0.22

vibrations due to intercalated carbonate ion (around 1360 cm^{-1}) and hydroxyl ions from layered hydroxides (around 3400 cm^{-1}) confirmed the successful formation of LDHs.[23] The weak vibration band at 1630 cm^{-1} is due to bending mode of the intercalated water molecules.[23]

Upon calcination at 400 °C, the formation of poorly crystallized mixed metal oxides is revealed by the PXRD patterns (Figure S2a). The characteristic peaks due to LDHs are no longer observed which indicates the collapse of the layered structure. Three broad reflections with *d*-values of 3.03 Å (2θ =29.4 °), 2.09 Å (2θ = 43.2 °) and 1.48 Å (2θ =62.7 °) were observed and are assigned to the Periclase MgO phase.[27] It is noteworthy to mention that no trace of aluminium oxides or other phases is observed from the PXRD pattern of all the samples. The characteristic vibrations of LDHs were significantly reduced on the FTIR spectra of MMOs (Figure S2b) and it suggests the formation of MMOs.[28] The weak 1400 and 1630 cm^{-1} bands are due to the adsorption of atmospheric moisture and CO_2 species.[28a,29] The vibration band below 1000 cm^{-1} became more intense, which indicates the formation of M–O bonding after calcination.

2.2. Crystal-chemical model of LDHs

The structural-composition relations for brucite-like hydroxides were first investigated on divalent metal hydroxides by Brindley *et al.*[30] and later extended to LDHs by Richardson[30–31] using a combination of geometrical arguments and crystal-chemical aspects. The models derived by Richardson demonstrate the posibility to calculate *x* from *a* for Ni- and Mg-based LDHs. To obtain the *x* of LDHs synthesized, the crystal-chemical model for Mg-based LDHs derived by Richardson was used (equation (1)). The *r* stands for ionic radii and α is the angle between metal cation and two oxygen sites of the same basal plane. For $r(Mg^{2+})$ and $r(Al^{3+})$ values, the Shannon's effective ionic radii of Mg^{2+} (0.72 Å) and Al^{3+} (0.53 Å) having the octahedral coordination were used.[25] The α and $r(OH^-)$ values employed here were the ones recommended by Richardson which are 97.41 ° and 1.365 Å, respectively.[31] It is important to point out that these values were obtained from wide-ranging sets of experimental *a*-parameters reported in the literature and their nominal *x* used at synthesis. Upon substitution of the above mentioned values for the different parameters in equation (1) and further rearrangement, equation (2) was derived.

$$a = 2\sin\frac{\alpha}{2}\left(r(Mg^{2+}) + r(OH^-)\right) - 2\sin\frac{\alpha}{2}\,x\left(r(Mg^{2+}) - r(Al^{3+})\right) \quad (1)$$

$$x = (3.133 - a)/0.2855 = 10.9737 - 3.5026a \quad (2)$$

By employing this equation and substituting the *a* values, the *x* values for the synthesized LDHs are obtained (Table 1). For simplicity's sake, this *x* value derived from Richardson's crystal-chemical model is denoted as $x_{crystal}$ and will be verified later. It is also important to remind that $x_{crystal}$ represents the actual Al content in the hydroxide layers and should not be confused with the $x_{nominal}$ which is nominal Mg: Al ratios used at synthesis.

As shown in Table 1, the *x* values derived from Richardson's model fall within the possible *x* range for LDHs phase (0.17 - 0.33). A narrow range of $x_{crystal}$ (0.22 - 0.28) is obtained and is close to the $x = 0.25$ observed for the LDH composition that is found in nature, the one of mineral hydrotalcite ($Mg_6Al_2CO_3(OH)_{16}{\cdot}4H_2O$). This suggests that synthetic LDHs tend to have a chemical composition that is close to the one for Hydrotalcite ($a = 3.054$ Å).[32] For instance, when attempts were made to synthesize LDHs with higher nominal *x* value (0.33) than that of Hydrotalcite, the composition tends to go towards $x = 0.25$ by intercalating lesser amount of Al^{3+} as evidenced by $x_{crystal}$ (0.28). Similarly, when synthesis of LDHs with lower *x* (0.17) was attempted, the observed $x_{crystal}$ is moving towards $x = 0.25$ (i.e. $x = 0.22$).

2.3. Elemental Analysis of LDHs

To verify $x_{crystal}$, the nominal (i.e. expected) concentration of metal ions in LDHs, which was calculated based on $x_{nominal}$, is compared with the observed (i.e. chemical) concentration obtained from elemental analysis (ICP-OES), $x_{chemical}$. From Table 2, a clear discrepancy between the expected and observed metal ion concentrations is seen, notably the Mg^{2+} concentrations, proved the deviation from the expected (nominal) composition. This is consistent with the larger $x_{crystal}$ values than the anticipated ones in all the samples, except for the sample synthesized with nominal Mg: Al ratio = 2 where it shows smaller $x_{crystal}$ value. This again shows that synthetic LDHs tend to have compositions that are not originally intended (nominal), and produce Hydrotalcite like composition ($x = 0.25$). On the other hand, no clear relationship between $x_{nominal}$ and the calculated $x_{chemical}$ is observed. For instance, the compositional deviation from the nominal value is relatively

Table 2. Nominal (expected) and observed (measured) concentration of LDHs measured from elemental analysis (ICP-OES).

Nominal Mg : Al ratios	Expected Concentration (wt %)		Observed Concentration (wt %)			$X_{nominal}$	$X_{crystal}$	$X_{chemical}$
	Mg	Al	Mg	Al	Na			
2	20.5	8.7	20.8	11.4	9.0	0.33	0.28	0.28
3	21.6	8.3	23.5	8.7	9.5	0.25	0.27	0.26
4	21.4	7.3	25.1	7.0	13.8	0.20	0.27	0.23
5	22.9	5.7	26.1	5.9	13.5	0.17	0.22	0.18

small in the case of LDHs with Mg: Al = 3 and 5 compared to the other two LDHs (Mg: Al = 2 and 4). In addition to the metal ions in LDHs, elemental analysis also revealed a significant amount of residual sodium in all samples, ranging between 9 to 14% (Table 2).

LDHs are known to crystallize only within a specific range of *x* (0.17 - 0.33). It is commonly believed that using nominal concentration of this range of *x* (0.17 – 0.33) yields pure LDHs. Whenever attempts were made to synthesize LDHs beyond this range, impurity phases were reported along with the LDHs.[21a,33] As described before, the $x_{chemical}$ calculated from chemical analysis does not distinguish between the metal cations in the LDHs crystal lattice and the ones in impurities. If impurity phases are formed, then elemental analysis includes them also as a part of total metal concentrations. In addition to that, some of the previously reported impurity phases, i.e. Al-based hydroxides/oxy-hydroxides, are amorphous in nature and hence are undetectable by PXRD measurements. To avoid such situation, in the present study only *x* within this range were used to synthesize LDHs but still resulted in a clear deviation between $x_{chemical}$ and $x_{crystal}$. This suggests the presence of phases other than LDHs. To address this potential presence of impurity phases, it is necessary to discuss the formation mechanism of LDHs.

The formation mechanism of LDHs is not as clearly established compared to their counterparts, cationic clays. The ambiguity falls between topotactic and dissolution-reprecipitation (D–R) mechanism, owing to the significant differences between solubility products (K_{sp}) of the unitary hydroxides present in LDHs. For instance, trivalent metal hydroxides ($K_{sp} = 10^{-31}$ - 10^{-38}) precipitates at a much lower pH (4 - 6) than the divalent metal hydroxides ($K_{sp} = 10^{-10}$ - 10^{-16}) that occurs above pH 8.[34] In an earlier study, Boclair *et al.* suggested LDHs are formed after the topotatic reaction between precipitated Al$(OH)_3$ and Mg^{2+} ions,[19a] whereas a later study from Radha *et al.* proposed a D–R mechanism, where the precipitated amphoteric Al$(OH)_3$ first dissolve and reprecipitated at higher pH along with magnesium hydroxide that forms LDHs.[19c] Since both topotactic or D–R mechanisms does not account for quantitative precipitation of the LDHs and they are qualitative in nature. On account of these discussions revolving around the formation mechanism of LDHs and the likely formation of amorphous Al^{3+} phases, we carried out solid-state ^{27}Al NMR to identify the aluminium phases present in samples.

2.4. Solid State ^{27}Al NMR of LDHs

Figure 1a presents the solid-state ^{27}Al NMR two dimensional (2D) MAS spectra for all the synthesized LDHs. The sharp peak close to δ *ca.* 9.3 ppm found in all spectra is assigned to the six-coordinated Al species (AlO_6) located at the octahedral sites of LDHs.[35] The chemical shifts for other coordination of Al^{3+} like AlO_5 (δ 30–35 ppm) and AlO_4 (δ 55–75 ppm) were not observed, which indicate the absence of these phases in the resultant LDHs. However, a closer look at the enlarged MAS spectra (Figure 1b) shows that the AlO_6 peak tails on both sides between 15 to –5 ppm, suggesting the potential presence of other AlO_6 species with chemical shifts that fall within the range, e.g. Gibbsite (6 & 8.3 ppm),[36] Bayerite (8.8 ppm),[36b] Boehmite (9.0 ppm)[37] and Pseudoboehmite (11.2 ppm).[38] It is also possible that the two other polymorphs of Al$(OH)_3$, Nordstrandite and Doyleite, also fall within this range but their solid-state ^{27}Al NMR information is not found in any literature. If any of the above mentioned phases precipitated as amorphous ones together with the LDHs, especially in minor quantities, it is difficult to identify these from the 2D NMR spectra due to the close resonance of the peaks.

To further interpret the NMR spectra, three-dimensional (3D) MQMAS spectra of LDHs were recorded (Figure 2). The clear shoulders extending from the centre at δ_2 *ca.* 10 ppm (δ_1 *ca.* 6 ppm), reaching towards lower δ_1 values of LDHs (i.e. −5 ppm) observed from all samples is consistent with the 2D MAS spectra above. This indicates the possibility of having Al^{3+} in other octahedral environment than LDHs. A similar observation has been previously reported by Rocha *et al.* but they attributed this difference in Al environment to the "random

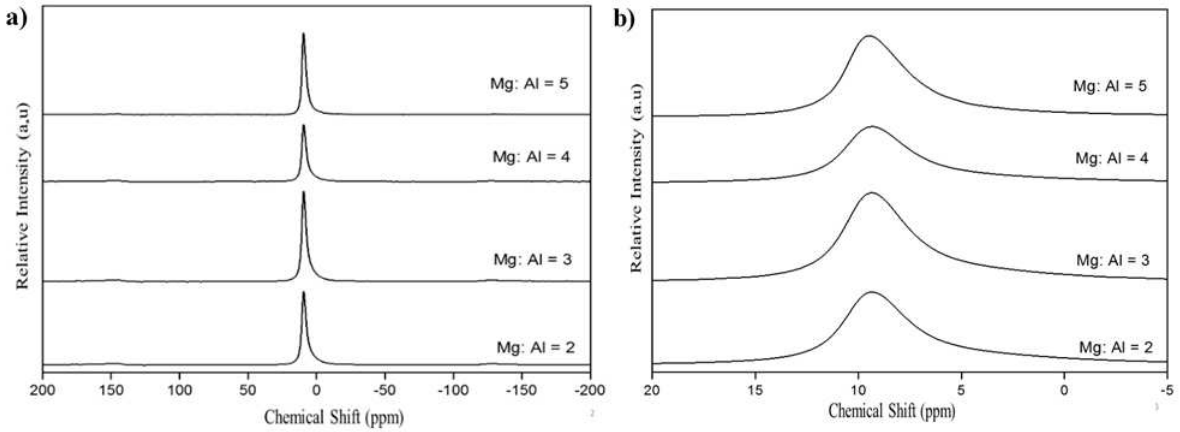

Figure 1. (a) full and (b) enlarged part (20 to −5 ppm) of solid-state ^{27}Al MAS NMR spectra of LDHs synthesized with different nominal Mg: Al ratios.

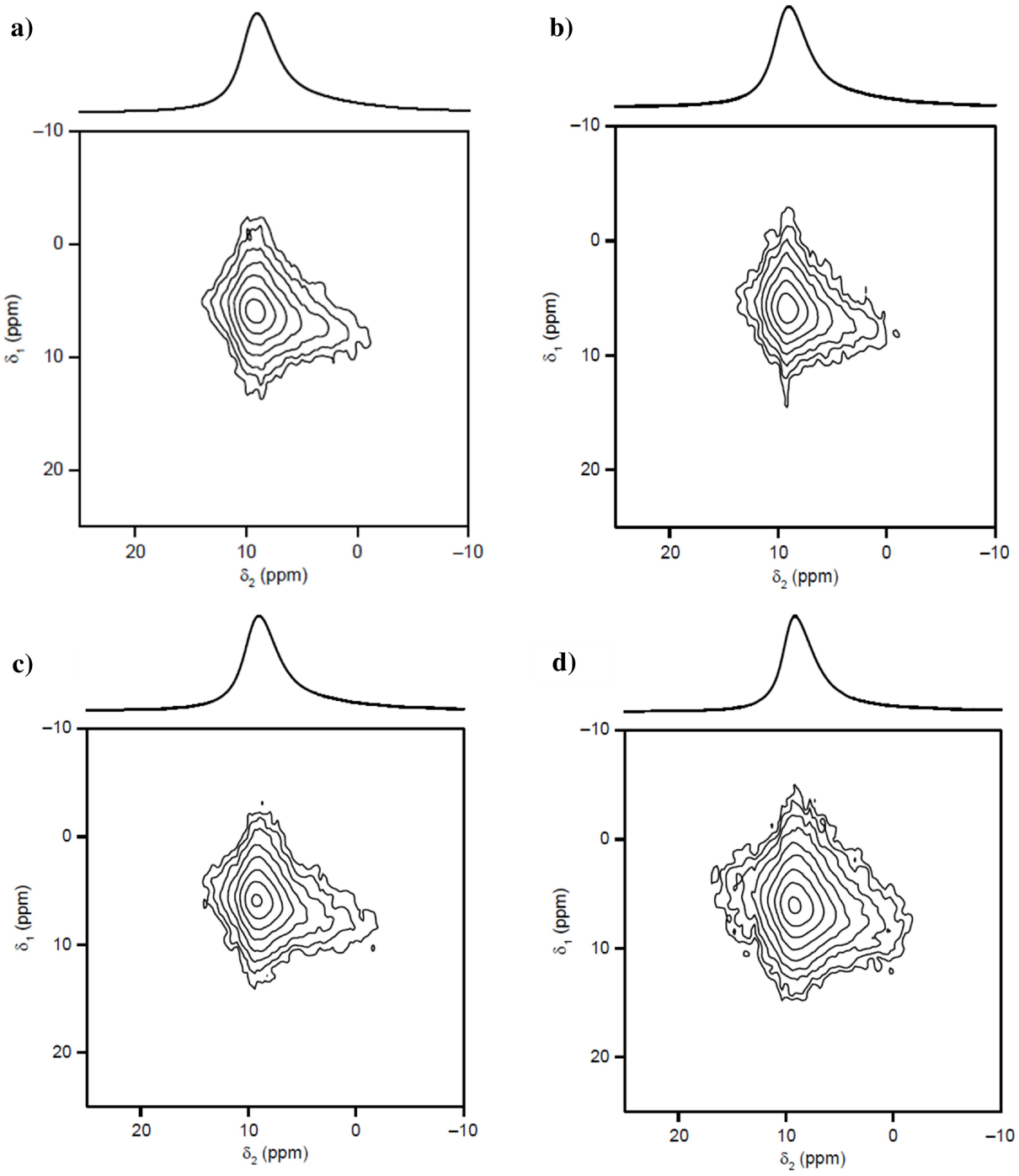

Figure 2. Solid-State ^{27}Al MQMAS NMR spectra of LDHs with nominal Mg: Al ratios of (a) 2, (b) 3, (c) 4 and (d) 5.

insertion of Al^{3+} in the layers".[39] The ordering of Al^{3+} within the LDHs hydroxide lattice has been extensively studied and is widely understood that the mutually repulsing Al^{3+} tends to locate as far as possible from each other with known ordering manner.[8] Based on this argument, random insertion of Al^{3+} into the crystal lattice is unlikely to occur. The same kind of observation was also obtained by Vyalikh *et al.*[40] To get a better understanding of the AlO_6 species present in LDHs, 2D NMR signals of all the LDHs were deconvoluted.

Figure 3 presents all the deconvoluted 2D NMR spectra of LDHs and the deconvoluted signals are tabulated in Table 3. Surprisingly, deconvolution shows that at least two additional resonances besides the one for LDHs (δ 9.3 ppm) are present in all samples. The chemical shifts obtained from deconvolution (δ 5.6, 5.8, 6.2, 8.5 and 8.6 ppm) are close match to those of Gibbsite, Bayerite and Boehmite. Given the complex solution chemistry during the formation of LDHs, precipitation of these phases as amorphous compounds is highly plausible. However,

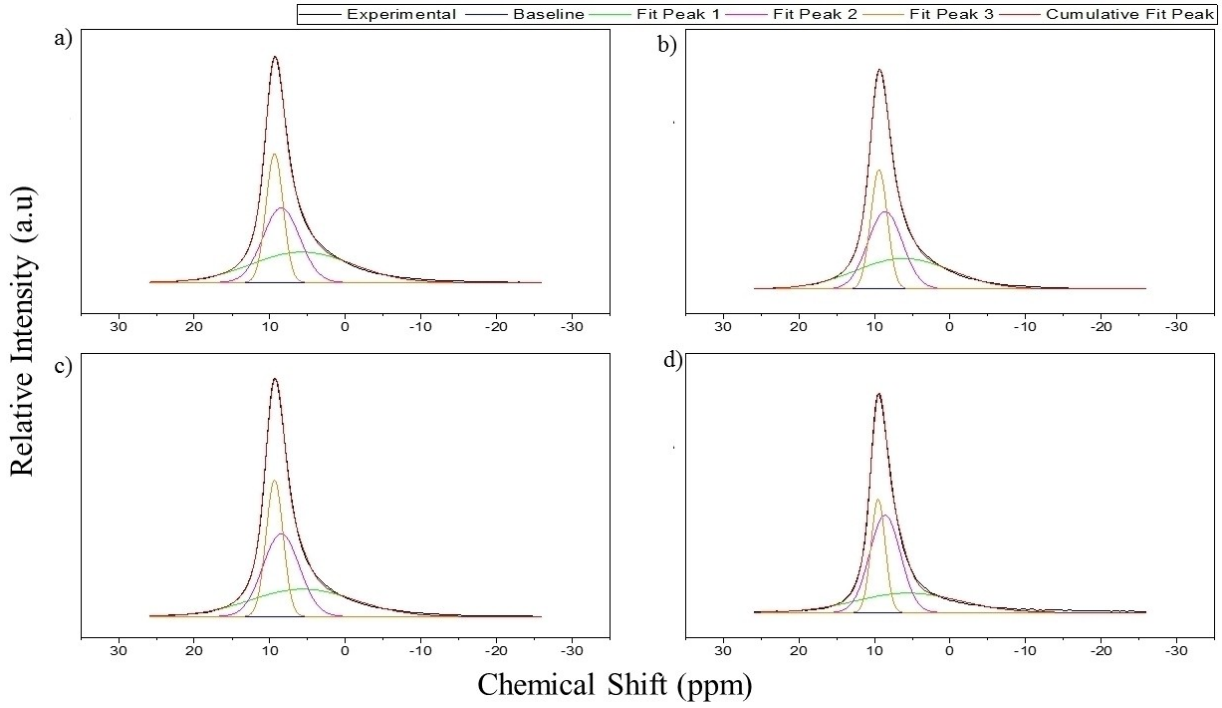

Figure 3. Solid-State ^{27}Al MQMAS NMR experimental and fit spectra of LDHs with nominal Mg: Al ratios of (a) 2, (b) 3, (c) 4 and (d) 5.

Table 3. Solid-state ^{27}Al MAS NMR chemical shifts obtained from deconvolution and fitness test.

Nominal Mg: Al ratios		2	3	4	5
Fitted Peak Signals (ppm)	I	5.8	6.2	5.6	5.6
	II	8.5	8.6	8.5	8.6
	III	9.4	9.4	9.4	9.5
Adj. R-Square		0.9995	0.9996	0.9995	0.9986

we are unable to assign these secondary phases to only one particular compound due to the overlapping chemical shifts of the abovementioned phases. Overall, ^{27}Al NMR data of LDHs shows the presence of secondary Al^{3+} phases as impurities, which is in line with the discrepancies observed in $x_{crystal}$ and $x_{chemical}$ values.

The 2D MAS spectra for all MMOs is included in Figure S3a. A new broad asymmetric line shape resonance emerged near 70 ppm suggests the presence of four-coordinated Al species (AlO_4). This is consistent with the previously reported movement of Al^{3+} from octahedral to tetrahedral sites in the MMOs lattice.[39] Interestingly, the AlO_6 peak of calcined LDHs synthesized with nominal Mg: Al ratio of 2 and 3 is visibly narrower (Figure S3b) compared to the two other samples, suggesting a more ordered and symmetric Al environment. This is in agreement with the result from elemental analysis as both samples showed the minimum deviation between $x_{chemical}$ and $x_{crystal}$.

When translated into 3D MQMAS, quite significant differences in spectra are observed across the samples. The most remarkable observation is the disappearance of AlO_4 resonance in the MQMAS spectra of MMOs samples with Mg: Al ratios of 3 (Figure S4b). However, this does not mean that four-coordinated Al species were not formed in the particular sample as the AlO_4 peak was clearly seen in 2D MAS (Figure 3a) and 3D MQMAS spectra (Figure 4b). We speculate that this is because of the large AlO_6 to AlO_4 ratio of the sample, which caused the AlO_4 intensity to virtually "disappear" from the spectrum. The obvious dissimilarities at the AlO_4 site across the samples also proved the presence of different Al phases.

2.5. CO_2 Adsorption

Figure 4a shows the CO_2 adsorption capacities of MMOs at 200 °C versus $x_{nominal}$, $x_{chemical}$ and $x_{crystal}$. There seems to be no obvious linear correlation between the composition of LDHs and CO_2 adsorption capacities of MMOs. Interestingly, the highest capacity (0.82 mmol/g) is measured from the MMOs having $x_{crystal}$ value of 0.27, rather than 0.22, which has a higher Mg content. In addition to that, three samples having very close $x_{crystal}$ values (0.27 - 0.29) were shown to have slightly different CO_2 adsorption capacities (0.69 - 0.82 mmol/g) which suggests a disputable relationship between them. Logically, materials of the same chemical composition and prepared by

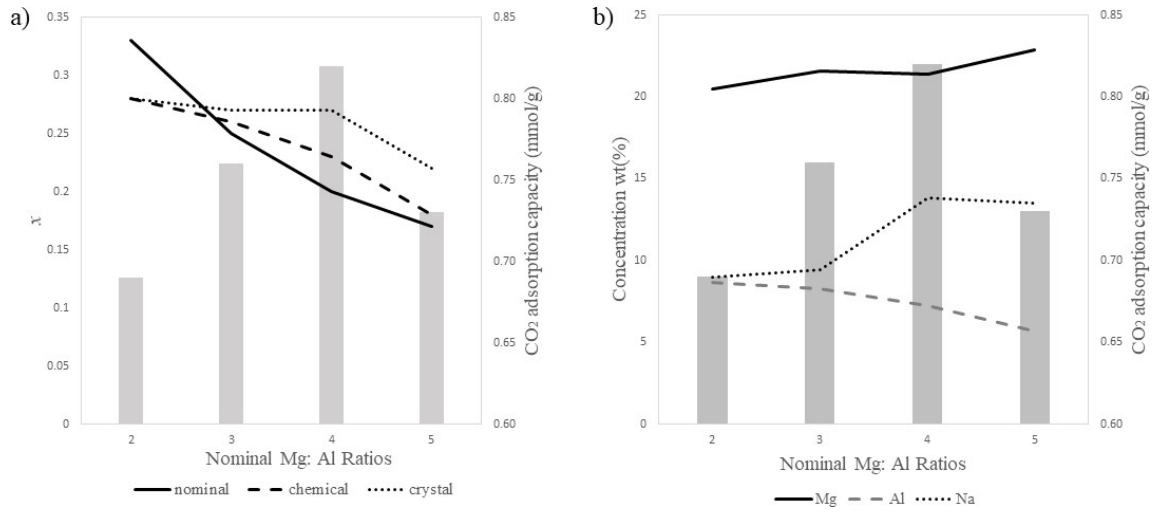

Figure 4. CO_2 uptake capacities of MMOs plotted with (a) x of LDHs and (b) concentration of metal cations obtained from ICP-OES.

the same synthesis method should exhibit similar properties. However, this is clearly not the case and this observation is similar to the previously reported results in the literature.[17] The impurity phases reported earlier in the present study may have played a role in the CO_2 capture capacities of MMOs.

The concentration of different metal ions obtained from elemental analysis is plotted against the observed CO_2 capture capacities in Figure 4b. Surprisingly, there is no direct relationship between the Mg^{2+} content of the samples and CO_2 capture capacities, as originally thought. However, there seems to be a trend between the amont of sodium present in each sample and the CO_2 capture capacity. For instance, the highest amount of sodium is present in LDHs with a nominal Mg: Al ratio of 4, which derived MMOs are the ones with the highest CO_2 capture capacity. Similarly, LDHs with a nominal Mg: Al ratio of 2 show the lowest amount of sodium and CO_2 capture capacity. This observation is in agreement with the strong basic nature of sodium which has previously been used in many studies to enhance CO_2 adsorption of MMOs.[41] However, the presence of sodium in all samples is somewhat intriguing. All the samples were synthesized according to the protocol reported in literature and washed with copious amount of water to remove excess sodium and metal salts used in the preparation.[7,9, 14, 17a, 42] The washing was stopped when the sample started to leach out or unsettle during the washing and is widely regarded as an indication to have removed all the excess chemicals used in the synthesis. In our washing step, we kept the washing water volume constant for all samples but it has resulted in huge differences in sodium content (9 – 14%) across the samples.

Complete removal of the sodium used in the synthesis of the LDHs is probably challenging due to the nature of the hydroxides involved, namely $Mg(OH)_2$ and $Al(OH)_3$. The excess post-synthesis washing of the LDHs brings down the pH of the filtrate close to neutral and at this pH, $Mg(OH)_2$ is thermodynamically unstable and becomes unsaturated.[43] Previous studies report LDHs that have been washed until the filtrate pH reaching 7 to remove excessive nitrate ions and sodium.[17a,21b, 44] But this could lead to the leaching out of the $Mg(OH)_2$ from LDHs phase leading to the partial dissolution of the LDHs.[22a] Hence, with the current washing technique, complete removal of sodium without affecting the composition of pristine LDHs seems difficult. This is likely the reason why inconsistent CO_2 adsorption capacities of LDHs (0.3 – 0.83 mmol/g) have been reported from different CO_2 capture studies, even though the materials were all prepared using the same synthesis method and nominal compositions.[14,17a,18]

Although we tried to establish a chemically meaningful relationship between the composition of LDHs and CO_2 adsorption of MMOs, however it is not as straightforward as it seems. There is no obvious direct relationship between the composition of LDHs and the CO_2 capture properties of their derived MMOs due to the presence of impurities and uncontrolled formation mechanisms involved. This new finding urged us to face the existence of impurities more seriously and understand that the handling of the sorbent material, starting from the synthesis method to applications, can affect the properties of the bulk samples.

3. Conclusions

The present work proposes to establish a chemically meaningful relationship between the Mg: Al ratio of precursor LDHs and the CO_2 adsorption capacities of derived MMOs sorbents. Synthetic LDHs with four different Mg: Al ratios (2, 3, 4, and 5) were synthesized *via* co-precipitation method and calcined at 400 °C to form MMOs that could capture CO_2 at high-temperature. Using a crystal-chemistry model and the lattice parameter *a*, the true composition of LDHs is obtained and a tendency to acquire the natural composition ($x = 0.25$) of the mineral Hydrotalcite was observed. Solid-state ^{27}Al NMR reveals the presence of Aluminum based hydroxide/oxyhydroxides as amorphous impurities in all the resultant LDHs. This study also demonstrates the necessity to combining crystal-chemistry

with analytical approaches in establishing the chemical compositions of LDHs. Elemental analysis shows a notable quantity of sodium content in all samples (9 - 14 wt %). The CO_2 capture capacity of MMOs derived from synthesized LDHs shows no direct correlation with established compositions of the LDHs. However, the CO_2 capture capacity seems to be more correlated with the amount of remnant sodium present in the samples. The sodium content in LDHs solution is highly inhomogeneous and uncontrollable even though all samples were handled with the same post-synthesis protocol. The presence of unavoidable impure phases in LDHs, especially the ones synthesized from co-precipitation method prompts us to examine its effects on CO_2 uptake more seriously in future studies.

Supporting Information Summary

The supporting information document consists of experimental details of the study, PXRD patterns of LDHs (Figure S1a) & MMOs (Figure S2a), FTIR spectra of LDHs (Figure S1b), MMOs (Figure S2b), solid-state ^{27}Al MAS NMR spectra of MMOs (Figure S3) and solid-state ^{27}Al MQMAS NMR spectra of MMOs (Figure S4).

Acknowledgments

The authors gratefully acknowledge the financial support from Engineering and Physical Sciences Research Council (EP/N024540/1) and James Watt Scholarship from Heriot-Watt University.

Conflict of Interest

The authors declare no conflict of interest.

Keywords: CO_2 Capture · Layered Double Hydroxides · Mixed Metal Oxides · Characterization · Impurity

[1] C. D. Keeling, S. C. Piper, T. P. Whorf, R. F. Keeling, *Tellus Ser. B* **2011**, *63*, 1–22.
[2] M. Bert, D. Ogunlade, d. C. Heleen, L. Manuela, M. Leo, *Carbon Dioxide Capture and Storage*, IPCC, Cambridge CB2 2RU ENGLAND, **2005**.
[3] B. Dutcher, M. Fan, A. G. Russell, *ACS Appl. Mater. Interfaces* **2015**, *7*, 2137–2148.
[4] T. O. Nelson, L. J. Coleman, P. Mobley, A. Kataria, J. Tanthana, M. Lesemann, L.-M. Bjerge, *Energy Procedia* **2014**, *63*, 6504–6516.
[5] N. D. Hutson, B. C. Attwood, *Adsorption* **2008**, *14*, 781–789.
[6] Z.-z. Yang, J.-j. Wei, G.-m. Zeng, H.-q. Zhang, X.-f. Tan, C. Ma, X.-c. Li, Z.-h. Li, C. Zhang, *Coord. Chem. Rev.* **2019**, *386*, 154–182.
[7] M. Ram Reddy, Z. Xu, a. G. Q Lu, J. Diniz da Costa, *Ind. Eng. Chem. Res.* **2008**, *47*, 2630–2635.
[8] a) G. Brindley, S. Kikkawa, *Am. Mineral.* **1979**, *64*, 836–843; b) I. Richardson, *Acta Crystallogr. Sect. B* **2013**, *69*, 629–633.
[9] S. Miyata, *Clay Clay Miner* **1980**, *28*, 50–56.
[10] U. Costantino, F. Marmottini, M. Nocchetti, R. Vivani, *Eur. J. Inorg. Chem.* **1998**, *1998*, 1439–1446.
[11] a) G. Manohara, *RSC Adv.* **2014**, *4*, 46126–46132; b) J.-M. Oh, S.-H. Hwang, J.-H. Choy, *Solid State Ionics* **2002**, *151*, 285–291.
[12] H. Nakayama, N. Wada, M. Tsuhako, *Int. J. Pharm.* **2004**, *269*, 469–478.
[13] U. Costantino, N. Coletti, M. Nocchetti, G. G. Aloisi, F. Elisei, *Langmuir* **1999**, *15*, 4454–4460.
[14] M. Ram Reddy, Z. Xu, G. Lu, J. Diniz da Costa, *Ind. Eng. Chem. Res.* **2006**, *45*, 7504–7509.
[15] a) D. Jansen, E. van Selow, P. Cobden, G. Manzolini, E. Macchi, M. Gazzani, R. Blom, P. P. Henriksen, R. Beavis, A. Wright, *Energy Procedia* **2013**, *37*, 2265–2273; b) G. Manzolini, E. Macchi, M. Gazzani, *Int. J GreenH Gas Con.* **2013**, *12*, 502–509; c) M. Gazzani, E. Macchi, G. Manzolini, *Fuel* **2013**, *105*, 206–219; d) N. N. Meis, J. H. Bitter, K. P. de Jong, *Ind. Eng. Chem. Res.* **2010**, *49*, 1229–1235; e) X. Zhu, S. Li, Y. Shi, N. Cai, *Prog. Energ. Combust.* **2019**, *75*, 100784.
[16] U. Sharma, B. Tyagi, R. V. Jasra, *Ind. Eng. Chem. Res.* **2008**, *47*, 9588–9595.
[17] a) Y. Gao, Z. Zhang, J. Wu, X. Yi, A. Zheng, A. Umar, D. O'Hare, Q. Wang, *J. Mater. Chem. A* **2013**, *1*, 12782–12790; b) Z. Yong, V. Mata, A. E. Rodrigues, *Ind. Eng. Chem. Res.* **2001**, *40*, 204–209.
[18] M. J. Ramírez-Moreno, I. C. Romero-Ibarra, M. A. Hernández-Pérez, H. Pfeiffer, *Ind. Eng. Chem. Res.* **2014**, *53*, 8087–8094.
[19] a) J. W. Boclair, P. S. Braterman, J. Jiang, S. Lou, F. Yarberry, *Chem. Mater.* **1999**, *11*, 303–307; b) R. kumar Allada, A. Navrotsky, H. T. Berbeco, W. H. Casey, *Sci. J.* **2002**, *296*, 721–723; c) A. Radha, P. V. Kamath, *Bull. of Mater. Sci.* **2003**, *26*, 661–666.
[20] J. W. Boclair, P. S. Braterman, *Chem. Mater.* **1999**, *11*, 298–302.
[21] a) J. Di Cosimo, V. Dıez, M. Xu, E. Iglesia, C. Apesteguıa, *J. Catal.* **1998**, *178*, 499–510; b) Q. Wang, H. H. Tay, Z. Guo, L. Chen, Y. Liu, J. Chang, Z. Zhong, J. Luo, A. Borgna, *Appl. Clay Sci.* **2012**, *55*, 18–26; c) R. Rothbauer, F. Zigan, *Z. Krist-Cryst Mater.* **1967**, *125*, 317–331.
[22] a) M. Jobbágy, A. E. Regazzoni, *Appl. Clay Sci.* **2011**, *51*, 366–369; b) S. Xu, M.-C. Liao, H.-Y. Zeng, X.-J. Liu, J.-Z. Du, P.-X. Ding, W. Zhang, *J. Inst. Chem.* **2015**, *56*, 174–180.
[23] F. Cavani, F. Trifiro, A. Vaccari, *Catal. Today* **1991**, *11*, 173–301.
[24] F. Zigan, R. Rothbauer, *Neu. Jb Mineral* **1967**, *1967*, 137À143.
[25] R. t Shannon, C. Prewitt, *Acta Crystallogr. Sect. B* **1970**, *26*, 1046–1048.
[26] L. Vegard, *Z. Phys.* **1921**, *5*, 17–26.
[27] R. M. Hazen, *Am. Mineral.* **1976**, *61*, 266–271.
[28] a) T. Hibino, Y. Yamashita, K. Kosuge, A. Tsunashima, *Clay Clay Miner.* **1995**, *43*, 427–432; b) W. Yang, Y. Kim, P. K. Liu, M. Sahimi, T. T. Tsotsis, *Chem. Eng. Sci.* **2002**, *57*, 2945–2953.
[29] N. Puttaswamy, P. V. Kamath, *J. Mater. Chem.* **1997**, *7*, 1941–1945.
[30] G. Brindley, C.-C. Kao, *Phys. Chem. Miner.* **1984**, *10*, 187–191.
[31] I. G. Richardson, *Acta Crystallogr. Sect. B* **2013**, *69*, 150–162.
[32] R. Allmann, H. Jepsen, *Neu. Jb Mineral* **1969**, *1969*, 544À551.
[33] M. C. Gastuche, G. Brown, M. M. Mortland, *Clay Miner.* **1967**, *7*, 177–192.
[34] D. Dobos, S. Wawzonek, *J. Electrochem. Soc.* **1976**, *123*, 348 C-348 C.
[35] K. J. MacKenzie, M. E. Smith, *Multinuclear solid-state nuclear magnetic resonance of inorganic materials, Vol. 6*, Elsevier, **2002**.
[36] a) K. MacKenzie, J. Temuujin, K. Okada, *Thermochim. Acta* **1999**, *327*, 103–108; b) R. Meinhold, R. Slade, R. Newman, *Appl. Magn. Reson.* **1993**, *4*, 121–140.
[37] K. MacKenzie, J. Temuujin, M. Smith, P. Angerer, Y. Kameshima, *Thermochim. Acta* **2000**, *359*, 87–94.
[38] R. C. Slade, T. W. Davies, *J. Mater. Chem.* **1991**, *3*, 361–364.
[39] J. Rocha, M. Del Arco, V. Rives, M. Ulibarri, *J. Mater. Chem.* **1999**, *9*, 2499–2503.
[40] A. Vyalikh, D. Massiot, U. Scheler, *Solid State Nucl. Magn. Reson.* **2009**, *36*, 19–23.
[41] a) Y. J. Min, S.-M. Hong, S. H. Kim, K. B. Lee, S. G. Jeon, *Korean J. Chem. Eng.* **2014**, *31*, 1668–1673; b) S. Kim, S. G. Jeon, K. B. Lee, *ACS Appl. Mater. Interfaces* **2016**, *8*, 5763–5767.
[42] a) N. N. Meis, J. H. Bitter, K. P. de Jong, *Ind. Eng. Chem. Res.* **2009**, *49*, 1229–1235; b) J. He, M. Wei, B. Li, Y. Kang, D. G. Evans, X. Duan, *Layered Double Hydroxides*, Springer Berlin Heidelberg, Berlin, Heidelberg, **2006**, pp. 89–119.
[43] C. Johnson, F. Glasser, *Clay clay miner.* **2003**, *51*, 1–8.
[44] M. León, E. Díaz, S. Bennici, A. Vega, S. Ordónez, A. Auroux, *Ind. Eng. Chem. Res.* **2010**, *49*, 3663–3671.

Submitted: November 21, 2019
Accepted: April 28, 2020